Title:

Nutrient limitation in surface water of the oligotrophic Eastern Mediterranean Sea: an enrichment microcosm experiment

Tsiola A.[1,2#], Pitta P.[1], Fodelianakis S.[2*], Pete R.[3], Magiopoulos I.[1,2], Mara P.[4], Psarra S.[1], Tanaka T.[5,6], Mostajir B.[3,7*]

Hellenic Centre for Marine Research, Institute of Oceanography, Heraklion Crete, Greece (1); University of Crete, Department of Biology, Heraklion Crete, Greece (2); Laboratoire d'Ecologie des Systèmes Marins Côtiers (ECOSYM), CNRS - Université Montpellier 2 & 1 – Ifremer - IRD, Montpellier, France (3); University of Crete, Department of Chemistry, Environmental Chemical Processes laboratory, Heraklion Crete, Greece (4); INSU-CNRS, Laboratoire d'Océanographie de Villefranche, Villefranche sur Mer cedex, France (5); Université Pierre et Marie Curie-Paris 6, Observatoire Océanologie de Villefranche, Villefranche sur Mer cedex, France (6); Centre d'Ecologie Marine Expérimentale MEDIMEER, Mediterranean Center for Marine Ecosystem Experimental Research, , CNRS - Université Montpellier 2, Montpellier-Sète, France (7)

Running Head: N P limitation in the Mediterranean: a microcosm study

 # Address correspondence to: Tsiola Anastasia, atsiola@hcmr.gr

Mailing address: Hellenic Centre for Marine Research (HCMR), Institute of Oceanography, Ex American Base Gournes, P.O. Box 2214, 71003 Heraklion, Crete, Greece. Phone: 00302810337713. Fax: 00302810337822.

*** Present address:**

Fodelianakis Stilianos: King Abdullah University of Science and Technology, Thuwal, Kingdom of Saudi Arabia

Behzad Mostajir: Marine Biodiversity, Exploitation and Conservation (MARBEC), UMR 9190, CNRS – Université de Montpellier –IFREMER – IRD, Montpellier, France

Abstract

The growth rates of planktonic microbes in the pelagic zone of the Eastern Mediterranean Sea are nutrient limited, but the type of limitation is still uncertain. During this study, we investigated the occurrence of N and P limitation among different groups of the prokaryotic and eukaryotic (pico-, nano-, and micro-) plankton using a microcosm experiment during stratified water column conditions in the Cretan Sea (Eastern Mediterranean). Microcosms were enriched with N and P (either solely or simultaneously) and the PO_4 turnover time, prokaryotic heterotrophic activity, primary production and the abundance of the different microbial components were measured. Flow cytometric and molecular fingerprint analyses showed that different heterotrophic prokaryotic groups were limited by different nutrients; total heterotrophic prokaryotic growth was limited by P, but only when both N and P were added, changes in community structure and cell size were detected. Phytoplankton were N and P co-limited, with autotrophic pico eukaryotes being the exception as they increased even when only P was added after a 2-day time lag. The populations of *Synechococcus* and *Prochlorococcus* were highly competitive with each other; *Prochlorococcus* abundance increased during the first two days of P addition but kept increasing only when both N and P were added, whereas *Synechococcus* exhibited higher pigment content and increased in abundance three days after simultaneous N and P additions. Dinoflagellates also showed opportunistic behavior at simultaneous N and P additions, in contrast to diatoms and coccolithophores, which diminished in all incubations. High DNA content viruses, selective grazing and the exhaustion of N sources probably controlled the populations of diatoms and coccolithophores.

Keywords: *Synechococcus, Prochlorococcus*, heterotrophic prokaryotes, viruses, eukaryotic phytoplankton

1. Introduction

Being at the base of all pelagic food webs, planktonic microbes regulate a plethora of oceanic processes and have a key role in global biogeochemical cycles. The long-term exploration of microbial life established the importance of microbes across all oceanic regimes [1]. Despite the large number of studies aimed at untangling the so-called "diversity-function" links, gaps in our understanding still exist, especially concerning the combined factors that shape complex microbial assemblages. The interplay between grazing, viral infection and the physico-chemical environment needs further investigation, starting with environments where planktonic microbes are particularly important; for instance, in oligotrophic environments [1]. The Eastern Mediterranean Sea (EMS) is an oligotrophic system that has been described as a "marine desert" [2] . It is a semi-enclosed basin characterized by anti-estuarine circulation. A gradient of increasing oligotrophy going eastwards [3] and a profoundly high N:P ratio in the deep layers are two of the basin's most unusual characteristics [4]. The gradient of oligotrophy can be traced in the low chlorophyll and productivity, the energy transfer to higher trophic levels, and organic matter production and accumulation [5, 6]. Triggered by the unusual Redfield ratio, several hypotheses have been put forward in order to explain the starvation patterns that illustrate the microbial components of the EMS. For instance, insufficient denitrification and N-rich atmospheric inputs [7] are mechanisms that might explain Redfield's N:P ratio in the deep waters of the EMS being ~28:1.

Oligotrophic environments are usually characterized by the dominance of pico- and nano-sized microbes [8] and the tight links between them [9]. Heterotrophic prokaryotes drive organic matter recycling and channel energy to higher trophic levels [10]. Due to their advantageously high cell surface-to-volume ratio, pico- and nano- sized microbes compete more efficiently for scarce nutrients than larger protists [11]. Despite this advantage, the growth of heterotrophic and autotrophic prokaryotes, as well as eukaryotic phytoplankton, is constrained in the EMS as PO_4 concentration is too low to allow its substantial diffusion into the cells [12], and other forms of phosphorus may not be bioavailable [13].

All nutrient-limitation scenarios depend on the balance between nutrient supply and demand of osmotrophs (organisms that uptake dissolved substrates), as well as on the ratio between the different nutrients. The consideration that EMS plankton is P-limited during the stratified period has been prompted by the non-typical Redfield ratio, and then supported by nutrient enrichment experiments [14]. Recent research, however, indicated that planktonic microbes experience nutrient limitation differently. For instance, in summer, heterotrophic prokaryotes (hereafter, HProk) are limited by P while phytoplankton is co-limited by N and P [15, 16]. A shift to other kinds of limitation of HProk (such as carbon limitation) has been proposed when

86 mineral nutrients are not sufficient for phytoplankton growth and organic carbon production
87 [17]. Moreover, several groups among HProk experience different degrees of P limitation as
88 some of them are adapted to constantly low nutrient concentration while others are better
89 competitors during episodic nutrient pulses, or capable of plasticity [18]. The general
90 limitation or co-limitation patterns become even more difficult to identify as they vary not
91 only among planktonic groups but also in spatiotemporal scales (e.g. seasons, coastal vs.
92 offshore, surface vs. deep waters) [e.g. references 12, 19–21]. In other words, while several
93 previous experiments aimed to unravel the nature of limitation (elemental type) of the
94 microbial components of the EMS at the community level, the heterogeneity of these
95 microbes has not been assessed.

96 Whatever the nature of the limitation, the competition and co-existence patterns created
97 within the microbial food web impact the pelagic system and the creation of ecological niches
98 [22, 23]. For instance, the quality of dissolved organic carbon accumulated in the surface
99 waters is controlled by the type of limitation, and controls the prokaryotic community
100 composition that utilizes it and, in turn, the metabolism of the whole community [21].

101 During the present study, a microcosm experiment was carried out in order to give new
102 insights into the limiting nutrient for different groups of the phytoplankton community and
103 HProk when the water column of the EMS was stratified and both nitrate and phosphate were
104 missing from the photic zone. Microcosms were enriched with N and P (either alone or
105 simultaneously); a high-resolution description of the biological system was given, and the
106 prokaryotic community composition was assessed by applying, for the first time
107 simultaneously, Denaturing Gradient Gel Electrophoresis (DGGE) and flow cytometry. The
108 abundance and diversity of all size fractions of the phytoplankton community were also
109 analyzed as well as production rates of HProk and PO_4 turnover time.

2. Materials & Methods

2. 1. Study site & Experimental setup

The microcosm experiment was performed with water from the oligotrophic Cretan Sea (Panagia Gulf, Dia Island, 35° 26.354' N 25° 13.202' E), during the stratified season, between 1st and 5th September, 2011. Low density polyethylene Nalgene bottles (10 L) were washed with acid (10% HCl) and rinsed with deionized water three times prior to setup. Bottles were then filled with non-filtered surface seawater collected 5 nautical miles north of Heraklion and were incubated in a land-based tank for 5 days (referred to as experimental Days 0-4) at ambient temperature (25°C). Three microcosms were enriched on Day 0 with nitrogen only (1.6 μM, in the form of NH_4Cl), three others with phosphorus only (1 μM, in the form of KH_2PO_4) and three more with nitrogen and phosphorus simultaneously, in the same forms and concentrations. The above-mentioned treatments are hereafter named as N+, P+, NP+, respectively. Three extra microcosms received no nutrient manipulation and served as control (hereafter named as K). The target concentration of added PO_4 was 100 nM, but we accidentally enriched with 1 μM, leading to Redfield's N:P ratio, in P+ and NP+ treatments, of 0.03:1 and 1.23:1, respectively. During the experiment, samples were taken from all twelve microcosms. Sampling frequency depended on the measurement. In order to avoid contamination, clean gloves were used during the preparation as well as sampling period. A screen was used to reduce intense incident light by 50%.

2. 2. Nutrients

Nutrient concentrations were measured on Day 0 (immediately after addition) and Day 4. NH_4 concentration was measured according to [24] and PO_4 according to [25]. The detection limits were 0.018 μM for phosphate and 0.019 μM for ammonium. Based on the measured concentrations, the consumption rate of each nutrient was estimated according to the (T0-T4)/(T0) ratio.

2. 3. Uptake of $^{33}PO_4$

The uptake rate of orthophosphate was measured using ^{33}P-orthophosphate [26]. Carrier-free ^{33}P-orthophosphate (PerkinElmer, 370 MBq ml^{-1}) was added to samples at a final concentration of 20-79 pM. Samples for the subtraction of the background and abiotic adsorption were fixed with 100% trichloroacetic acid (TCA) before isotope addition. Samples were incubated under subdued (laboratory) illumination. The incubation time varied between 10 and 120 minutes, in order to be short enough to assure a linear relationship between the fraction of isotope adsorbed vs. the incubation time, and long enough to reliably detect

isotope uptake above background levels. Incubation was stopped by a cold chase of 100 mM KH_2PO_4 (final concentration 1 mM). Subsamples on Day 0 were filtered in parallel onto 25 mm polycarbonate filters with 0.2 µm pore size. All filters were placed on a Millipore 12-place manifold with Whatman (GF/C) glass fiber filters saturated with 100 mM KH_2PO_4 as support. After filtration, filters were placed in polyethylene scintillation vials with the scintillation cocktail and radio-assayed. Radioactivity of the filter was corrected for the blank filter obtained from fixed samples, and then phosphate turnover time ($T_{(PO4)}$ in hours) was calculated as $T_{(PO4)} = -t/\ln(1-f)$, where f is the fraction (no dimension) of added isotope collected on the 0.2 µm filter after the incubation time (t in hours).

2. 4. Prokaryotic Heterotrophic Activity and Primary production

Prokaryotic heterotrophic activity (PHA) was assayed on Days 0, 2 and 4 by the ^{3}H-thymidine, and on Day 4 by the ^{3}H-leucine incorporation methods, according to the micro-centrifuge methods of [27] and [28], respectively. For $PHA_{thymidine}$, working solutions of 500 µCi mL^{-1} (^{3}H)-thymidine stock solutions (Amersham Life Science, U.K.) were used, previously stored in the dark at 4°C. Prior to PHA, saturation experiment were performed to determine which concentration of isotope was required to swamp natural isotope levels. For each experimental microcosm, 250 ml samples were drawn in 250 ml polycarbonate bottles darkened with thick tape. Isotope labeling was done in two sets of five 2-ml micro-centrifuge tubes containing 1.4 ml of seawater samples. Five tubes were spiked with (^{3}H)-thymidine to a final concentration of 78 nM and five tubes were spiked with L-(4,5-^{3}H)leucine to a final concentration of 10 nM. Each set of micro-centrifuge tubes included two killed controls with 89 µl 100% TCA (background) and 3 tubes for incubations. The tubes were incubated in the dark in a thermo-regulated incubator at seawater temperatures for 4 hours. At the end of the incubation, 89 µL of 100% TCA were added to terminate prokaryotic heterotrophic production. The samples were spun at 16000 rpm for 10 min. After centrifugation, the supernatant was carefully removed and discarded. Then 1.7 ml of ice-cold 5% TCA was added to each tube, the solution was vortexed and the centrifugation step was repeated. At the end of the second centrifugation, the TCA supernatant was removed and replaced with 1.7 ml of ice-cold 80% ethanol. The solution was vortexed once again and centrifuged for a third time then the ethanol supernatant was removed. Finally, each tube received 1 ml of Ultima Gold XR scintillation cocktail (Packard Bioscience, N.L.) and final vortexing. The micro-centrifuge tubes were placed inside 20 ml glass scintillation vials and radio-assayed in a scintillation counter (Tricarb, Packard) to measure disintegrations per minute (DPM). Conversion of DPM to thymidine incorporated as carbon was done using thymidine

conversion factors of $2x10^{-18}$ cell per mole of thymidine incorporated and thymidine to carbon conversion factor of 20 fg thymidine $cell^{-}$ [29].

Total primary production (PP_t) was estimated on Days 0, 2 and 4, by the ^{14}C incorporation method, according to [30]. Two light and one dark 320-ml polycarbonate bottles were filled with water from the microcosms in the morning, inoculated with 5 µCi of $NaH^{14}CO_3$ tracer and incubated in the land-based tank for approximately 3 hours. The incubations were generally done around midday, when incident light was at its greatest, thus yielding maximum PP_t rates. The incubation area received the same light intensity as the microcosm bottles. At the end of the incubation time, replicate bottles were immediately filtered through 0.2, 2.0 and 5.0 µm 47 mm polycarbonate filters. All filtrations were performed under low vacuum pressure. In order to remove excess ^{14}C-bicarbonate, filters were soaked in 1 ml 0.1 N HCl and left in open polyethylene 5-ml vials overnight. After adding 4 ml of scintillation cocktail, radioactivity was measured in a Packard TriCarb 2100 scintillation counter; 0.2-2.0 µm, 2.0-5.0 µm and >5.0 µm fractions corresponded to pico-, small nano- and large nano- and micro-planktonic PP_t rates, respectively (hereafter, $PP_{0.2\text{-}2.0}$, $PP_{2.0\text{-}5.0}$, $PP_{>5.0}$) and were obtained by the respective subtraction between the related filters, while >0.2 µm represented total PP_t. For the concentration of dissolved inorganic carbon, the value 24000 mg C m^{-3} was used [31]. For the isotopic discrimination factor, the value 1.05 was used.

2. 5. Abundance of microbial components

Abundance of virus-like-particles (VLP), heterotrophic prokaryotes (HProk), cyanobacteria (including *Synechococcus* and *Prochlorococcus*) and autotrophic pico eukaryotes was estimated daily by flow cytometry. A FACS Calibur (Becton Dickinson) instrument was used, equipped with an air-cooled laser at 488 nm and standard filter setup. Samples for VLP and HProk counts were fixed with 0.2 µm-pre filtered 25% glutaraldehyde (0.5% final concentration). Fixed samples were kept at 4°C for approximately 30 minutes then deep frozen in liquid nitrogen and stored at -80°C until enumeration. Cryotubes were thawed at room temperature then stained with SYBR Green I nucleic acid dye, according to [32] and [33] for VLP and HProk enumeration, respectively. Briefly, VLP were stained with SYBR Green I (finally diluted $5x10^{-5}$ of the stock solution) and incubated at 80°C for 10 minutes. HProk were stained with SYBR Green I (finally diluted $4x10^{-4}$ of the stock solution) and incubated for 10 minutes in the dark. Cyanobacteria and autotrophic pico eukaryotes were analyzed without fixation and staining throughout the experiment. Flow cytometry data were acquired and processed with the Cell Quest software (Becton Dickinson). A standard and calibrated flow rate was used for all calculations (58 µl min^{-1} for high speed performance). Sub-groups of VLP and HProk were determined according to SYBR Green I fluorescence

intensity of particles. Samples for micro-phytoplankton enumeration were fixed in alkaline Lugol solution on Days 0, 2 and 4 and stored at 4°C in the dark. Subsamples (100 ml) were concentrated with the use of settling chambers, according to [34] and examined after 24 hours under an inverted microscope (Olympus, IX 70).

2. 6. Prokaryotic community composition

Samples for Prokaryotic Community Composition (PCC) assessment were collected on Day 0 from two control microcosms (before any nutrient addition) and Day 4 from all microcosms. For each sample, two liters of seawater were used for DNA extraction following a phenol-chloroform extraction method modified version of the method of [35], as described elsewhere [36]. The average quantity of recovered DNA per sample was 5 μg. PCC was assessed through DGGE of PCR-amplified fragments of the V3 hyper-variable region of the 16S rRNA locus, as described in [37].

2. 7. Statistical analyses

Statistical analysis was conducted on SPSS software. Student t-test was applied in order to compare values of a given parameter between the beginning and the end of the experiment. One-way analysis of variance (ANOVA) was applied in order to test the effect of each treatment on a given parameter on Day 4 only. Furthermore, repeated measures ANOVA was applied in order to compare a given parameter between treatments across the experimental period. Post hoc Tukey honestly significant difference test (Tukey HSD) was performed after the ANOVA test ($p<0.05$ was considered significant).

For PCC, cluster analysis (Average Linkage Hierarchical Clustering) was performed based on the Bray-Curtis index, which was calculated from the presence/absence DGGE data in PRIMER 6 for Windows. The significance of the clustering was calculated using 999 random permutations.

3. Results

3.1. Nutrients

On Day 0, NH_4 varied between 0.01 µM and 0.05 µM in K and P+ microcosms. In these treatments, NH_4 was fully consumed by the end of the experiment (Fig. 1a). In N+ and NP+ treatments, NH_4 was 1.71 ± 0.05 µM on Day 0 and showed differential consumption patterns until Day 4. While in N+ treatment only a minor part of the added NH_4 was consumed (~3%), in NP+ treatment half or more of the added NH_4 was consumed (~49%), as derived by the (Day 0-Day 4)/(Day 0) concentration ratio. PO_4 was below the detection limit of the analytical method in K and N+ microcosms during all experimental days. In P+ and NP+ treatments, immediately after addition PO_4 was 1.39 µM (Fig. 1b), and it was consumed more in P+ than in NP+ treatment (~8 and ~4%, respectively). The concentration of PO_4 added accidentally deviated from the originally planned one, possibly driving the system into severe N limitation in the P+ and NP+ microcosms, as derived by the resulting extremely low N:P ratio (approximately 1).

3.2. PO_4 turnover time

A short turnover time (<7 hours) was observed in K and N+ treatments throughout the experimental period, as well as at initial conditions in P+ and NP+ treatment (Fig. 1c). A pronounced increase in PO_4 turnover time was observed when PO_4 was added either alone or together with NH_4 (Tukey HSD, $p<0.05$) immediately after addition. PO_4 turnover time peaked on Day 1 in the NP+ treatments, reaching values two orders of magnitude higher than in K (Fig. 1c). In contrast, PO_4 turnover time in the P+ treatment also reached high values on Days 1, 3 and 4, which even exceeded the maximum values recorded in NP+ treatments. In both K and N+ incubations, on Day 1 there was a slight decrease of PO_4 turnover time (1-2 hours), and the values remained at these levels until Day 4.

3.3. Prokaryotic Heterotrophic Activity and Primary Production

$PHA_{thymidine}$ in the N+ treatment followed exactly the same trend as in K, with constantly low rates (Fig. 1d). The addition of PO_4 alone influenced $PHA_{thymidine}$, which experienced an increase on Day 2 followed by a decrease on Day 4 to rates 30-fold higher than the respective ones in K microcosms (Tukey HSD, $p<0.05$). When NH_4 and PO_4 were added simultaneously, a statistically significant increase in $PHA_{thymidine}$ compared to the controls, N+ and P+ (Tukey HSD, $p<0.01$), was observed. On Day 4, $PHA_{thymidine}$ in the NP+ treatment was two orders of magnitude higher than in the controls (Fig. 1d). $PHA_{leucine}$ measurements on Day 4 also showed a significant increase only when both N and P were added (Fig. 1e). $PHA_{leucine}$

was significantly different between N+ and P+ treatments on Day 4 (Tukey HSD, $p<0.05$). The ratio between $PHA_{leucine}/PHA_{thymidine}$ ranged between 0.004 and 0.04 on Day 4, with the lowest values observed in the controls and the highest ones in the NP+ incubations (Fig. 2).

Similarly to PHA, PP followed exactly the same trend in the N+ treatment as in K, with constantly low rates (Fig. 1f). In contrast to PHA, PP exhibited a slight decrease on Day 2, which was then followed by a reset to initial values. Only when both nutrients were added was an increase (10-fold) observed (Tukey HSD, $p<0.05$). All size fractions of PP followed consistent trends in time. $PP_{0.2\text{-}2.0}$ was initially dominant in all treatments (approx. 65%) while $PP_{2.0\text{-}5.0}$ and $PP_{>5.0}$ contributed equally in N+, P+ and NP+ incubations at initial conditions (Fig. 3a). The $PP_{0.2\text{-}2.0}$ dominance shifted towards larger phytoplankton groups on Day 4 in K and NP+ microcosms (Fig. 3b, Tukey HSD, $p<0.05$) while in N+ and P+ treatments, there was no consistent trend between the replicates. On Day 4, the contribution of $PP_{0.2\text{-}2.0}$ in NP+ microcosms was significantly higher than that in K microcosms.

3.4. Abundance of microbial components

Starting from an initial abundance of $1.7x10^4$ cells ml^{-1}, *Synechococcus* increased in the K and N+ treatments on Day 1, peaked on Day 2 and then decreased until Day 4 (Fig. 4a). In contrast, in the P+ and NP+ treatments, *Synechococcus* abundance first decreased (Day 1), then continuously increased until Day 4 (NP+) or dropped after Day 3 (P+); however, there was no statistical difference between P+ and NP+ treatments throughout the experiment (Tukey HSD, $p>0.05$). On Day 2, *Synechococcus* cells in all microcosms appeared in two groups (data not shown). However, on Days 3 and 4, this phenomenon was apparent only in K and N+ microcosms. *Synechococcus* cells with significantly higher phycoerythrin content (approx. 3-4x higher) characterized NP+ treatment on Days 3 and 4 (data not shown).

Prochlorococcus cells were apparent in all microcosms from the beginning of the experiment (Fig. 4b) in very low numbers ($3.9x10^4$ cells ml^{-1}). The abundance of this group progressively diminished in K and N+ treatments only. *Prochlorococcus* abundance in the NP+ treatment slightly decreased on Day 1 and then continuously increased until Day 4. In contrast, in the P+ treatments it increased until Day 2 and then dropped. However, and due to variability among replicates, there was no statistically significant difference between the P+ and NP+ incubations (Tukey HSD, $p>0.05$).

Autotrophic pico eukaryotes did not oscillate until Day 2 in any incubation (Fig. 4c). From Day 3, there was a distinct and significant difference between K and N+, and P+ and NP+ treatments. While in the former treatments autotrophic pico eukaryotic abundance remained

constant, in the latter ones it increased sharply and significantly (Tukey HSD, $p<0.05$). Autotrophic pico eukaryotes were favored when PO_4 was added, either alone or simultaneously with NH_4, on Day 4 (Tukey HSD, $p<0.05$), but reached higher values at the NP+ treatment.

HProk were equally favored by either PO_4 alone or NH_4 and PO_4 simultaneous additions (Tukey HSD, $p>0.05$). N+ treatment followed exactly the same trend as K throughout the experiment, and P+ followed the exact same trend as NP+ (Fig. 4d). The highest HProk abundances ($8.6x10^5$ cells ml^{-1}) were observed in both P+ and NP+ treatments on Day 3. In all three NP+ microcosms, a population of larger HProk, based on higher side scatter fluorescence, was apparent from Day 1 (data not shown). VLP followed the same pattern of HProk (Fig. 4e), showing a significant peak in P+ and NP+ incubations, which was particularly high on Day 3. In K and N+ incubations, VLP remained constant, with slight oscillations towards lower values on the first two days.

According to SYBR Green I fluorescence level, HProk were separated into two groups, characterized by low and high DNA content (hereafter, $HProk_{low}$ and $HProk_{high}$, respectively). At initial conditions, $HProk_{low}$ and $HProk_{high}$ contributed equally to the community of all microcosms (Fig. 5); however, between Day 0 and Day 4, a statistically significant difference in the $HProk_{low}/HProk_{high}$ ratio was observed in P+ and NP+ microcosms (t-tests, $p=0.003$ and $p<0.001$, respectively) and $HProk_{high}$ dominated on Day 4 in these treatments. VLP were separated into three groups, characterized by low, medium and high DNA content; hereafter, VLP_{low}, VLP_{medium} and VLP_{high}, respectively (Fig. 5). The proportion of VLP_{low} significantly increased on Day 4, similarly in P+ and NP+ treatments (t-test, $p=0.01$ and $p<0.001$, respectively). VLP_{high} always constituted a minor part of the viral community but significantly increased between Days 0 and 4 in all incubations, except for N+ (t-test, $p>0.05$).

Total nano- and micro- phytoplankton abundance decreased or remained constant in all treatments from Day 0 to Day 4, except for NP+ microcosms, where a significant increase in abundance was observed in some cases (Tukey HSD, $p<0.05$). More specifically, all major phytoplankton groups (diatoms, dinoflagellates and coccolithophores) remained constant throughout the experimental time in K (Fig. 4f-h). In the nutrient-amended microcosms, phytoplankton groups exhibited different patterns. On one hand, dinoflagellates, that formed 99% of both abundance and biomass of phytoplankton and were represented by >80% by small *Gymnodinium* species (<20μm) decreased in N+ and P+ treatments to half or less of their initial value, but they significantly increased in NP+ ($p<0.05$) due to several-fold increases of small *Gymnodinium* species (Fig. 4g). On the other hand, diatoms decreased to half of their initial abundance in N+ treatments and completely diminished at P+ and NP+

(Fig. 4f). Lastly, coccolithophores remained stable in N+ and P+ treatments, similar to K, but decreased in NP+ only (Fig. 4h). However, significant results for coccolithophores abundance were not obtained as abundance in the NP+ replicates was highly variable. On the same time, it has to be noted that coccolithophores and diatoms (essentially represented by the genera Coccolithus, Emiliania, and Thalassiothrix, Navicula, Hemialus, respectively) together occupied less than 1% of phytoplankton abundance and biomass.

3.5. Prokaryotic Community Composition

Although total operational taxonomic unit (OTU) richness was not affected by any of the enrichments (non-parametric t-tests, n=3, $p>0.05$ for all tests), significant shifts were observed in the community composition of various samples. Four sample clusters were significant (Fig. 6): cluster A, with 87.7% average similarity containing the samples from *in situ* C1 and C2, K1 and K2 on Day 4 and three N+ microcosms on Day 4 microcosms; cluster B, with 91.7% average similarity containing the samples from three P+ microcosms; cluster C, containing two NP+ microcosms (NP2 and NP3) and showing 25% dissimilarity from all other samples; and cluster D, with 75.4% average similarity containing samples from K3 and NP1 microcosms. The latter cluster was the most dissimilar compared to the other three, possibly showing that these samples acted as outliers (Fig. 7). The clustering of the rest of the samples indicated that, on one hand, N addition induced non-detectable changes in the prokaryotic community, but on the other hand, P addition induced slight-yet-detectable changes. However, the most profound changes were detected after the addition of both N and P.

4. Discussion

In this study, we aimed to assess the occurrence of P and/or N and P co-limitation in the oligotrophic EMS during stratified conditions by consolidating in a microcosm experiment most of the microbial components (from viruses and heterotrophic prokaryotes up to pico-, nano- and micro- phytoplankton). Seawater enclosures have been extensively and successfully used as an experimental tool that links natural habitats with controlled conditions [38], providing the opportunity to answer specific ecological questions at multiple levels of the microbial food web. During this experiment, N and P concentrations were manipulated in microcosms filled with surface offshore water from the EMS, initially characterized by undetectable P levels and ultra-oligotrophic conditions (Table 1) typical for the end-of-summer period [39].

PO_4 turnover time is the first indication of P depletion and a particularly useful measurement in oligotrophic environments where P concentration is close to or below the detection limit of the analytical methods [12, 40]. In our experiment, PO_4 turnover time was low and behaved similarly in K and N+ microcosms, indicating that P was deficient and osmotrophs were P-limited, as observed in similar experiments [12, 14, 41]. However, PO_4 turnover time is a measurement of PO_4 availability only and it does not exclude the possibility that some (or all) osmotrophs are limited by other substrates too.

Among osmotrophs, the heterotrophic prokaryotic community in particular was found to be primarily P-limited and this was indicated not only by PO_4 turnover time but also by HProk abundance, and it is in accordance with past microcosm and mesocosm experiments in the Mediterranean Sea [12, 15, 18]. Furthermore, the measurements of $PHA_{leucine}$ revealed that single P addition significantly increased HProk activity compared to the microcosms that received N or no nutrients. However, when both N and P were added, the incorporation of leucine into HProk was more pronounced, agreeing with the findings of a similar microcosm experiment carried out in offshore waters of the EMS [16]. Consequently, our results underline that the heterotrophic prokaryotic community was ultimately co-limited by N and P. The $PHA_{leucine}/PHA_{thymidine}$ ratio [42] indicates whether growth of prokaryotes on a given system is balanced or unbalanced, with a ratio of <1 indicating unbalanced growth where DNA synthesis occurs at higher rates than protein synthesis [43]. In our experiment, this ratio was <1 (0.004 - 0.04), showing unbalanced growth of HProk, which was more pronounced in K treatments compared to NP+.

In order to further clarify the response of heterotrophs to nutrient additions, prokaryotic community composition was assessed. A significant increase in $HProk_{high}$ from Day 0 to Day

4 in both P+ and NP+ incubations implied that highly active HProk [44] dominated the community after enrichment with P. The tight link between $PHA_{thymidine}$ and $HProk_{high}$ in these two treatments (Pearson's correlation, r^2=0.778, p<0.01, n=15) but not in K and N+ proved that $HProk_{high}$ group was responsible for the increased productivity, as seen elsewhere [45]. Only a minor part of N was consumed when it was added alone, and all microbial components behaved similarly to the control microcosms. While HProk abundance slightly increased in the controls and N+, the overall community composition remained stable and there was no significant difference in the % contribution of HProk members. Moreover, a distinct population with higher SSC signal in the flow cytometry fluorescence plots was developed from Day 1 in NP+ and implied that N and P simultaneous enrichment caused additional alterations in the heterotrophic community, indicating a link with the pronounced PHA increase in NP+ treatment. Similar responses of the prokaryotic community towards cells of larger sizes have been observed in previous experiments under P-stressed conditions [46, 47]. In the oligotrophic subtropical North Atlantic Sea, large prokaryotes accounted for the majority of bacterial biomass in NP+ treated microcosms despite the fact that they were less abundant, as was also the case in our study [48]. This shift is often typified as an advantageous and opportunistic mechanism of P-limited osmotrophs in order to store nutrients in excess [49], successfully avoid ingestion by predators [50] and simultaneously increase competitiveness for nutrient uptake [51]. Phenotypic variation towards large (*size*) and elongated (*shape*) forms of prokaryotic cells might be also related to a higher protein content and could have been followed by another shift towards larger grazers, e.g. ciliates. P addition to the nutrient-limited waters of the EMS has led to an increase of HProk activity, which was subsequently channeled to higher trophic levels without an increase in phytoplankton biomass [15, 52]. In our experiment, heterotrophic flagellates and ciliates abundance was not measured but certainly these microbes played a key role in the system, as suggested by similar experiments where the added nutrients were quickly transferred from bacteria to ciliates through heterotrophic nano-flagellates [e.g. 41].

Further to the flow cytometric assessment of HProk, changes in prokaryotic community composition (PCC) according to DGGE were significant when P was added either solely or along with N. However, the simultaneous N and P addition had the most pronounced impact on PCC, potentially reflecting the alterations in the % of active cells (common between P+ and NP+) and the appearance of large HProk cells (only in NP+). Different HProk lineages that experience different types of limitation have been also found in nutrient-amendment studies with higher-resolution analytical techniques [18, 36]. DGGE analysis is a molecular fingerprint technique that allows taxonomic assessments in a relatively low resolution and roughly depicts prokaryotic community diversity alterations, possibly masking some minor

ones. However, it is assumed to be a useful approach for monitoring the evolution of prokaryotic assemblages [e.g. 53, 54]. The PCC did not differentiate when N was added alone, confirming that N was either non-limiting or its addition was not sufficient to enhance growth of prokaryotes, as previously mentioned in related studies [36, 55].

The phytoplankton community seemed to have more complicated responses to the nutrient enrichments. On Day 4, while *Synechococcus* and *Prochlorococcus* abundance responded positively to simultaneous additions only (suggesting N and P co-limitation), autotrophic pico eukaryotes seemed to be only P-limited. In previous experiments, *Synechococcus* as well as the total phytoplankton community responded to simultaneous N and P enrichments, proposing that N or P alone was not adequate for assimilation and growth [16]. During that microcosm experiment, as well as during a larger-scale Lagrangian experiment [41], no response or a decline of autotrophic pico eukaryotes to P additions, respectively, were observed. In our study, these cells increased at both P+ and NP+ after a time lag of two days. The discrepancy between our study and other related ones could imply that autotrophic pico eukaryotes accessed lower levels of the nitrogen pool or were benefited by the high P addition. An increase in cellular pigment content of autotrophic pico-plankton after simultaneous N and P additions has been reported [16] and, in our experiment too, cells of higher phycoerythrin and chlorophyll content characterized *Synechococcus* during Days 3 and 4 only in the NP+ incubations. Sole P addition did not stimulate cyanobacterial growth as expected [56], probably due to severe N limitation driven by the high P input and the resulting low N:P ratio.

When considering Day 4, indeed *Synechococcus* and *Prochlorococcus* seemed to be N and P co-limited. However, on a temporal scale, all microcosms exhibited shifts in the "cyanobacterial" level, with the two major players showing opposing responses. On one hand, *Synechococcus* appeared in two populations in all microcosms on Day 2 but remained in this form only in K and N+ microcosms until Day 4. It has been previously shown that P and N additions affect the cell cycle of cyanobacteria [57]. As a result, the presence of the separated forms of *Synechococcus* might depict dividing cells. The two distinct populations could also depict different *Synechococcus* strains, which are often found in the Mediterranean waters and depend on ambient P concentrations [58]. On the other hand, *Prochlorococcus* cells were apparent in low numbers from the beginning of the experiment, typical of the sampling depth and season. *Prochlorococcus* immediately diminished in K and N+ microcosms only, implying that they were probably outcompeted by *Synechococcus* cells in these microcosms. In contrast, when P was added (both in P+ and NP+), *Prochlorococcus* abundance increased, possibly taking advantage of the inability of *Synechococcus* to compete efficiently for

463 inorganic P when in excess, compared to smaller pico- sized prokaryotes (HProk and
464 *Prochlorococcus*), which apparently increased rapidly at that time. Unlike our results, past
465 research [16, 52] showed that *Prochlorococcus* completely disappeared from all incubations
466 irrespective of the nutrients added. It seems that when P was added in our microcosms,
467 *Prochlorococcus* and HProk were the first to respond, despite evidence that *Synechococcus*
468 have superior affinities for PO_4 than HProk and eukaryotic algal cells [59]. Competition for P
469 between *Prochlorococcus* and HProk [19] could have shaped the community after Day 2, as
470 well as the competition between *Synechococcus* and pico- eukaryotes [60].

471 PCC changes observed only in the NP+ incubations may also be associated with the fact that
472 phytoplankton and DOM composition largely affects prokaryotes [61]. Indeed, nano- and
473 micro- phytoplankton growth was co-limited by N and P, and the compositional shifts in this
474 group after nutrient enrichment possibly provided additional substrates for prokaryotic growth
475 [10]. Dinoflagellates significantly increased in NP+ incubations, implying opportunistic
476 behavior, whereas diatoms diminished, contrary to the notion that diatoms usually benefit
477 from rapid or sporadic nutrient pulses [62]. N and P enrichment might have led to increased
478 density-dependent grazing upon diatoms [63]. Additional "pressure" on diatoms could
479 originate from viruses, as NP+ microcosms diatom abundance declined and VLP_{high}
480 simultaneously and significantly increased. Laboratory-based studies showed that VLP_{high}
481 infect and cause high mortality in eukaryotic phytoplankton [64], with an increasing pressure
482 after blooming. Extensive phytoplankton losses due to viral lysis could also have occurred in
483 our experiment in the non-nutrient-limited incubations, as it has been shown that viral
484 replication is constrained under inorganic nutrient limitation [65] and P addition causes an
485 induction of prophages [66]. Finally, as diatoms need and acquire more N than P [67], they
486 probably became N-limited after consuming the added amount of nitrogen in NP+, resulting
487 in additional stress upon them. The extremely low N:P ratio in P+ and NP+ microcosms (due
488 to the error in P addition, i.e. higher than the related protocols) might have obscured the
489 growth of several phytoplanktonic taxa that became strongly N-limited, in contrast to
490 previous studies that showed that phytoplankton exhibited increased growth rates under single
491 P addition [e.g. 56].

492 Under nutrient-limited conditions, planktonic microbes of small size fractions are expected to
493 dominate and coexist [68]. Co-existence can be achieved by exhibiting different types of
494 limitation, expressing mixotrophic behavior and acquiring phenotypic and genotypic
495 alterations [9, 50, 69] in order to minimize competition and utilize nutrients to their maximum
496 [70]. In the surface EMS waters, where the majority of the growth-limiting labile nutrients are
497 supplied through episodic Saharan dust events [71], it is important to better understand how

498 the trophic links are affected by nutrient enrichment. The results of our study confirm that
499 heterotrophic and autotrophic microorganisms may primarily compete for the same nutrient
500 (i.e. P) and secondly for another one (i.e. N), as observed in several marine ecosystems over
501 time and space [e.g. 72]. We showed that N and P additions caused a shift towards increased
502 total autotrophic biomass, as previously seen in the Mediterranean [73], and further that
503 different components of HProk and phytoplankton were limited by different substrates. Some
504 of the most complex and diverse patterns of nutrient limitation were detected within
505 autotrophs (*Synechococcus* vs. *Prochlorococcus*, pico vs. nano- and micro- eukaryotic
506 phytoplankton) and within heterotrophs (different prokaryotic lineages). Similar diverse
507 responses among trophic groups resemble dust-enrichment microcosm and mesocosm
508 experiments [74, 75]; on one hand, bacteria exhibited rapid increase in growth rate and
509 alterations in the species-level (driven by P availability), and on the other hand,
510 phytoplankton showed variable responses mainly according to their size and physiological
511 characteristics. Sole P addition had a positive impact on HProk growth, but it was not
512 sufficient to cause compositional changes, as well as a positive impact on autotrophic pico
513 eukaryotes, however not as strong as that after simultaneous N and P addition. Clearer
514 responses were seen on larger phytoplankton: dinoflagellates were limited by N and P and
515 seemed to remain unaffected by losses until the end of the experiment, while diatoms and
516 coccolithophores vanished from all incubations, possibly due to extensive grazing and viral
517 attack, and the exhaustion of available nutrients (mainly strong N limitation). In our study, we
518 also observed taxonomic and phenotypic alterations in the NP+ incubations (with the most
519 pronounced being a shift towards highly pigmented and larger/more active cells, seen in
520 *Synechococcus* and HProk, respectively) that have a critical role in the presence and selective
521 predation/infection of grazers/viruses, and ultimately the channeling of energy to higher
522 trophic groups in the oligotrophic EMS. Based on nitrate and phosphate measurements the
523 EMS microbial ecosystem in summer is assumed to be N and P co-limited. However, our
524 results showed that the actual pattern is more complex, as the type and extent of limitation
525 was highly variable within phytoplankton and HProk; as a result, it is of great value to focus
526 on individual planktonic groups of the microbial food web in order to identify their limiting
527 nutrient(s).

Acknowledgements

This work was funded by the European Union Framework Program (FP7/2007-2013), grant agreement N° 228224, MESOAQUA project. We thank the captain and the crew of *R/V Philia*, as well as Panagiotis Vavilis and Dimitris Apostolakis for their help at sea. We also wish to thank Frede T. Thingstad for his suggestions on the experimental design, as well as Tatiana M. Tsagaraki for her invaluable support in microcosm assembling and advice on statistical analysis. Thanks are also due to Snezana Zivanovic and Eleni Dafnomili for conducting nutrient analyses and Ioannis Tsakalakis for help with primary production measurements. Finally, we thank Sebastian Mas, Emilie Le Floc'h and other members of MEDIMEER and ECOSYM teams for the installation and running of the mesocosm experiment on the new transportable floating *in situ* mesocosm platform with autonomous sensors deployed in the Cretan Sea in September 2011, simultaneously to the present investigation.

References

1. Karl DM (2007) Microbial oceanography: paradigms, processes and promise. Nature 5:759-769.

2. Azov Y (1991) Eastern Mediterranean- a marine desert? Mar Poll Bull 23:225-232.

3. Moutin T, Raimbault P (2002) Primary production, carbon export and nutrients availability in western and eastern Mediterranean Sea in early summer 1996 (MINOS cruise). J Mar Syst 33-34:273–288. doi: 10.1016/S0924-7963(02)00062-3.

4. Krom MD, Emeis KC, Van Cappellen P (2010) Why is the Eastern Mediterranean phosphorus limited? Prog Oceanogr 85:236–244. doi: 10.1016/j.pocean.2010.03.003.

5. Turley CM, Bianchi M, Christaki U, Conan P, Harris JRW, Psarra S, Ruddy G, Stutt ED, Tselepides A, Van Wambeke F (2000) Relationship between primary producers and bacteria in an oligotrophic sea- the Mediterranean and biogeochemical implications. Mar Ecol Prog Ser 193:11-18.

6. Moutin T, Thingstad TF, Van Wambeke F, Marie D, Slawyk G, Raimbault P (2002) Does competition for nanomolar phosphate supply explain the predominance of the cyanobacterium *Synechococcus*? Limnol Oceanogr 47(5):1562-1567.

7. Krom MD, Herut B, Mantoura RFC (2004) Nutrient budget for the Eastern Mediterranean: Implications for phosphorus limitation. 49:1582–1592. doi: 10.4319/lo.2004.49.5.1582.

8. Wassmann P, Ypma JE, Tselepides A (2000) Vertical flux of faecal pellets and microplankton on the shelf of the oligotrophic Cretan Sea (NE Mediterranean Sea). Prog Oceanogr 46:241–258. doi: 10.1016/S0079-6611(00)00021-5.

9. Hartmann M, Grob C, Tarran GA, Martin AP, Burkill PH, Scalan DJ, Zubkov VM (2012) Mixotrophic basis of Atlantic oligotrophic ecosystems. Proc Natl Acad Sci USA 109(15):5756-5760.11. Fouilland E, Mostajir B (2010) Revisited phytoplanktonic carbon dependency of heterotrophic bacteria in freshwaters, transitional, coastal and oceanic water. FEMS Microbiol Ecol 73:419-429. doi: 10.1073/pnas.1118179109.

10. Fouilland E, Mostajir B (2010) Revisited phytoplanktonic carbon dependency of heterotrophic bacteria in freshwaters, transitional, coastal and oceanic waters. FEMS Microbiol Ecol 73:419–429. doi: 10.1111/j.1574-6941.2010.00896.x.

11. Koch AL (1996) What size should a bacterium be? A question of scale. Annu Rev Microbiol 50:317–348. doi: 10.1146/annurev.micro.50.1.317

573 12. Tanaka T, Thingstad TF, Christaki U, Colombet J, Cornet-Barthaux V, Courties C,
574 Grattepanche J-D, Lagaria A, Nedoma J, Oriol L, Psarra S, Pujo-Pay M, Van Wambeke F
575 (2011) Lack of P-limitation of phytoplankton and heterotrophic prokaryotes in surface waters
576 of three anticyclonic eddies in the stratified Mediterranean Sea. Biogeosciences 8:525-538.

577 13. Gilbert JA, Thomas S, Cooley NA, Kulakova A, Field D, Booth T, McGrath JW, Quinn JP,
578 Joint I (2009) Potential for phosphonoacetate utilization by marine bacteria in temperate coastal
579 waters. Environ Microbiol 11(1):111-125. doi: 10.1111/j.1462-2920.2008.01745.x

580 14. Zohary T, Robarts RD (1998) Experimental study of microbial P limitation in the eastern
581 Mediterranean. Limnol Oceanogr 43:387–395. doi: 10.4319/lo.1998.43.3.0387

582 15. Thingstad TF, Krom MD, Mantoura RFC, Flaten GAF, Groom S, Herut B, Law CS, Pasternak
583 A, Pitta P, Psarra S, Rassoulzadegan F, Tanaka T, Tselepides A, Wassmann P, Woodward
584 EMS, Wexels Riser C, Zodiatis G, Zohary T (2005) Nature of phosphorus limitation in the
585 ultraoligotrophic Eastern Mediterranean. Science 309:1068-1071. doi:
586 10.1126/science.1112632

587 16. Zohary T, Herut B, Krom MD, Mantoura, RFC, Pitta P, Psarra S, Rassoulzadegan F, Stambler
588 N, Tanaka T, Thingstad TF, Woodward EMS (2005) P-limited but N and P co-limited
589 phytoplankton in the Eastern Mediterranean- a microcosm experiment. Deep Sea Res Part 2
590 Top Stud Oceanogr 52:3011-3023. doi: 10.1016/j.dsr2.2005.08.011

591 17. Kirchman D (1994) The uptake of inorganic nutrients by heterotrophic bacteria. Microb Ecol
592 28:255–271.

593 18. Sebastián M, Gasol JM (2013) Heterogeneity in the nutrient limitation of different
594 bacterioplankton groups in the Eastern Mediterranean Sea. ISME J 7:1665–8. doi:
595 10.1038/ismej.2013.42

596 19. Sala MM, Peters F, Gasol JM, Pedrós-Alió C, Marrasé C, Vaqué D (2002) Seasonal and spatial
597 variations in the nutrient limitation of bacterioplankton growth in the northwestern
598 Mediterranean. Aquat Microb Ecol 27:47-56. doi: 10.3354/ame027047.

599 20. Van Wambeke F, Christaki U, Giannakourou A, Moutin T, Souvemerzoglou K (2002)
600 Longitudinal and vertical trends of bacterial limitation by phosphorus and carbon in the
601 Mediterranean Sea. Microbial Ecol 43:119-133. doi: 10.1007/s00248-001-0038-4.

602 21. Pinhassi J, Gómez-Consarnau L, Alonso-Sáez L, Sala MM, Vidal M, Pedrós-Alió C, Gasol JM
603 (2006) Seasonal changes in bacterioplankton nutrient limitation and their effects on bacterial
604 community composition in the NW Mediterranean Sea. Aquat Microb Ecol 44:241-252. doi:
605 10.3354/ame044241.

606 22. Thingstad TF (2000) Elements of a theory for the mechanisms controlling abundance,
607 diversity, and biogeochemical role of lytic bacterial viruses in aquatic systems. Limnol
608 Oceanogr 45(6):1320–1328. doi: 10.4319/lo.2000.45.6.1320.

609 23. Gifford SM, Sharma S, Booth M, Moran MA (2012) Expression patterns reveal niche
610 diversification in a marine microbial assemblage. ISME J 7:281–298. doi:
611 10.1038/ismej.2012.96.

612 24. Ivančič I, Deggobis D (1984) An optimal manual procedure for ammonia analysis in natural
613 waters by the indophenol blue method. Water Res 18:1143–1147. doi: 10.1016/0043-
614 1354(84)90230-6.

615 25. Strickland JDH, Parsons TR (1972) Determination of phosphorus. *In* Strickland JDH, Parsons
616 TR. (ed), A Practical Handbook of Seawater Analysis, 2nd ed, Bulletin No 167, Fisheries
617 Research Board of Canada. Ottawa.

618 26. Thingstad TF, Skjoldal EF. Bohne RA (1993) Phosphorus cycling and algal-bacterial
619 competition in Sandsfjord, western Norway. Mar Ecol Prog Ser 99:239-259. doi:
620 10.3354/meps099239.

621 27. Kirchman DEK (2001) Measuring bacterial biomass production and growth rates from leucine
622 incorporation in natural aquatic environments, p. 227-237. *In* Paul JH (ed), Marine
623 microbiology. Methods in microbiology, vol 30, St Petersburg, Florida, USA.

624 28. Smith S, Azam F (1992) A simple economical method for measuring bacterial protein synthesis
625 rates using 3Leucine. Marine Microbial Food Webs 6:170-114.

626 29. Fukuda R, Ogawa H, Nagata T, Koike I (1998) Direct determination of carbon and nitrogen
627 contents of natural bacterial assemblages in marine environments. Appl Environ Microb
628 64(9):3352-3358.

629 30. Steemann Nielsen E (1952) The use of radioactive carbon (^{14}C) for measuring organic
630 production in the sea. Jour Conseil 18:117-140.

631 31. Copin-Montegut C (1993) Alkalinity and carbon budgets in the Mediterranean sea. Global
632 Biogeochem Cy 4:915–925.

633 32. Marie D, Brussaard CPD, Thyrhaug R, Bratbak G, Vaulot D (1999) Enumeration of marine
634 viruses in culture and natural samples by flow cytometry. Appl Environ Microb 65(1):45-52.

635 33. Marie D, Partensky F, Jacquet S, Vaulot D (1997) Enumeration and cell cycle analysis of
636 natural populations of marine picoplankton by flow cytometry using the nucleic acid stain
637 SYBR Green I. Appl Environ Microbiol 63:186–193.

638 34. Utermöhl H (1958) Zur Vervollkommung der quantitativen phytoplankton methodik. Mitt
639 Internat Verein Limnol 9:1-38.

640 35. Massana R, Murray AE, Preston CM, DeLong EF (1997) Vertical distribution and
641 phylogenetic characterization of marine planktonic Archaea in the Santa Barbara Channel.
642 Appl Environ Microbiol 63(1):50–56.

643 36. Fodelianakis S, Pitta P, Thingstad TF, Kasapidis P, Karakassis I, Ladoukakis ED (2014*a*)
644 Phosphate addition has minimal short-term effects on bacterioplankton community structure of
645 the P-starved Eastern Mediterranean. Aquat Microb Ecol 72:98-104. doi: 10.3354/ame01693

646 37. Fodelianakis S, Papageorgiou N, Karakassis I, Ladoukakis ED (2015) Community structure
647 changes in sediment bacterial communities along an organic enrichment gradient associated
648 with fish farming. Ann Microbiol 65:331–338. doi: 10.1007/s13213-014-0865-4.

649 38. Taub FB (1997) Unique information contributed by multispecies systems: examples from the
650 standardized aquatic microcosm. Ecol Appl 7(4):1103-1110.

651 39. Siokou-Frangou I, Christaki U, Mazzocchi MG, Montresor M, Ribera d' Alcalá M, Vaqué D,
652 Zingone A (2010) Plankton in the open Mediterranean Sea: a review. Biogeosciences 7:1543-
653 1586. doi: 10.5194/bg-7-1543-201.

654 40. Moutin T, Karl DM, Duhamel S, Rimmelin P, Raimbault P, Van Mooy BAS, Claustre H
655 (2008) Phosphate availability and the ultimate control of new nitrogen input by nitrogen
656 fixation in the tropical Pacific Ocean. Biogeosciences Discuss 4:2407–2440. doi: 10.5194/bgd-
657 4-2407-2007.

658 41. Pitta P, Stambler N, Tanaka T, Zohary T, Tselepides A, Rassoulzadegan F (2005) Biological
659 response to P addition in the Eastern Mediterranean Sea. The microbial race against time. Deep
660 Res Part II Top Stud Oceanogr 52:2961–2974. doi: 10.1016/j.dsr2.2005.08.012.

661 42. Chin-Leo G, Kirchman DL (1990) Unbalanced growth in natural assemblages of marine
662 bacterioplankton. Mar Ecol Prog Ser 63:1-8. doi: 10.3354/meps063001.

663 43. Gasol JM, Alonso-Sáez L, Vaqué D, Baltar F, Calleja ML, Duarte CM, Arístegui J (2009)
664 Mesopelagic prokaryotic bulk and single-cell heterotrophic activity and community
665 composition in the NW Africa-Canary Islands coastal-transition zone. Prog Oceanogr 83:189-
666 196. doi: 10.1016/j.pocean.2009.07.014

667 44. Gasol JM, Zweifel UL, Peters F, Fuhrman JA, Hangstrom Å (1999) Significance of size and
668 nucleic acid content heterogeneity as measured by flow cytometry in natural plankton bacteria.
669 Appl Environ Microb 65(10):4475-4483.

670 45. Bonilla-Findji O, Herndl GJ, Gattuso J-P, Weinbauer G (2009) Viral and flagellate control of
671 prokaryotic production and community structure in offshore Mediterranean waters. Appl
672 Environ Microb 75(14):4801-4812. doi: 10.1128/AEM.01376-08.

673 46. Ovreås L, Bourne D, Sandaa R-A, Casamayor EO, Benlloch S, Goddard V, Smerdon G, Heldal
674 M, Thingstad TF (2003) Response of bacterial and viral communities to nutrient manipulations
675 in seawater mesocosms. Aquat Microb Ecol 31:109-121. doi: 10.3354/ame031109

676 47. Sebastián M, Pitta P, González JM, Thingstad TF, Gasol JM (2012) Bacterioplankton groups
677 involved in the uptake of phosphate and dissolved organic phosphorus in a mesocosm
678 experiment with P-starved Mediterranean waters. Environ Microbiol 14:2334-2347. doi:
679 10.1111/j.1462-2920.2012.02772.x

680 48. Mills MM, Moore CM, Langlois R, Milne A, Achterberg E, Nachtigall K, Lochte K, Geider
681 RJ, La Roche J (2008) Nitrogen and phosphorus co-limitation of bacterial productivity and
682 growth in the oligotrophic subtropical North Atlantic. Limnol Oceanogr 53(2):824-834. doi:
683 10.4319/lo.2008.53.2.0824.

684 49. Martin P, Dyhrman ST, Lomas MW, Poulton NJ, Van Mooy BAS (2014) Accumulation and
685 enhanced cycling of polyphosphate by Sargasso Sea plankton in response to low phosphorus.
686 Proc Natl Acad Sci USA 111(22):8089-8094. doi: 10.1073/pnas.1321719111.

687 50. Matz C, Jürgens K (2003) Interaction of nutrient limitation and protozoan grazing determines
688 the phenotypic structure of a bacterial community. Microb Ecol 45:384–398. doi:
689 10.1007/s00248-003-2000-0.

690 51. Tammert H, Lignell R, Kisand V, Olli K (2012) Labile carbon supplement induces growth of
691 filamentous bacteria in the Baltic Sea. Aquat Biol 15:121–134. doi: 10.3354/ab00424.

692 52. Krom MD, Thingstad TF, Brenner S, Carbo P, Drakopoulos P, Fileman TW, Flaten GAF,
693 Groom S, Herut B, Kitidis V, Kress N, Law CS, Liddicoat MI, Mantoura RFC, Pasternak A,
694 Pitta P, Polychronaki T, Psarra S, Rassoulzadegan F, Skjoldal EF, Spyres G, Tanaka T,
695 Tselepides A, Wassmann P, Wexels Riser C, Woodward EMS, Zodiatis G, Zohary T (2005).
696 Summary and overview of the CYCLOPS P addition Lagrangian experiment in the Eastern
697 Mediterranean. Deep Res Part II Top Stud Oceanogr 52:3090-3108.

698 53. Schäfer H, Bernard L, Courties C, Lebaron P, Servais P, Pukall R, Stackebrandt E, Troussellier
699 M, Guindulain T, Vives-Rego J, Muyzer G (2001) Microbial community dynamics in the

700 Mediterranean nutrient-enriched sweater mesocosms: changes in the genetic diversity of
701 bacterial populations. FEMS Microbiol Ecol 34:243-253.

702 54. Cleary FR, Smalla K, Mendonca-Hagler LCS, Gomes NCM (2012). Assessment oof variaiton
703 in bacterial composition among microhabitats in a mangrove environment using DGGE
704 fingerprint and barcoded pyrosequencing. PLoS 7(1):1-8. doi: 10.1371/journal.pone.0029380

705 55. Joint I, Henriksen P, Fonnes GA, Bourne D, Thingstad TF, Riemann B (2002) Competition for
706 inorganic nutrients between phytoplankton and bacterioplankton in nutrient manipulated
707 mesocosms. Aquat Microb Ecol 29:145-159.

708 56. Psarra S, Zohary T, Krom MD, Mantoura FC, Polychronaki T, Stambler N, Tanaka T,
709 Tselepides A, Thingstad TF (2005). Phytoplankton response to a Lagrangian phosphate
710 addition in the Levantine Sea (Eastern Mediterranean). Deep Res Part II Top Stud Oceanogr
711 52:2944-2960.

712 57. Vaulot D, Nebot N, Marie D, Fukai E (1996) Effect of phosphorus on the *Synechococcus* cell
713 cycle in surface Mediterranean waters during summer. Appl Environ Microb 62(7):2527-2533.

714 58. Lasternas S, Agustí S, Duarte CM (2010) Phyto- and bacterioplankton abundance and viability
715 and their relationship with phosphorus across the Mediterranean Sea. Aquat Microb 60:175-
716 191. doi: 10.3354/ame01421.

717 59. Tanaka T, Rassoulzadegan F, Thingstad TF (2003) Measurements of phosphate affinity
718 constants and phosphorus release rates from the microbial food web in Villefranche Bay,
719 northwestern Mediterranean. Limnol Oceanogr 48(3):1150-1160. doi:
720 10.4319/lo.2003.48.3.1150.

721 60. Dolan JR, Thingstad TF, Rassoulzadegan F (1996) Phosphorus transfer between microbial
722 size-fractions in Villefranche Bay (North Western Mediterranean Sea), France, in autumn
723 1992. Ophelia 41(1):15–22.

724 61. Arrieta J, Herndl GJ (2002) Changes in bacterial β-glucosidase diversity during a coastal
725 phytoplankton bloom. Limnol Oceanogr 47:594–599. doi: 10.4319/lo.2002.47.2.0594.

726 62. Allen AE, Dupont CL, Oborník M, Horák A, Nunes-Nesi A, McCrow JP, Zheng H, Johnson
727 DA, Hu H, Fernie AR, Bowler C (2011) Evolution and metabolic significance of the urea cycle
728 in photosynthetic diatoms. Nature 473:203-209.

729 63. Kang HK, Poulet S, Ju SJ (2007) Direct examination of the dietary preference of the copepod
730 *Calanus helgolandicus* using the colorimetric approach. Ocean Sci J 42(3):193–197. doi:
731 10.1007/BF03020923.

64. Brussaard CPD, Short SM, Frederickson CM, Suttle CA (2004*b*) Isolation and phylogenetic analysis of novel viruses infecting the phytoplankton *Phaeocystis globosa* (Prymnesiophyceae). Appl Environ Microb 70(6):3700-3705. doi: 10.1128/AEM.70.6.3700-3705.2004.

65. Wilson WH, Mann NH (1997) Lysogenic and lytic viral production in marine microbial communities. Aquat Microb Ecol 13:95–100. doi: 10.3354/ame013095

66. Boras JA, Sala MM, Vázquez-Domínguez E, Weinbauer MG, Vaqué D (2009) Annual changes of bacterial mortality due to viruses and protists in an oligotrophic coastal environment (NW Mediterranean). Environ Microbiol 11(5):1181-1193.

67. Tantanasarit C, Englade AJ, Babel S (2013) Nitrogen, phosphorus and silicon uptake kinetics by marine diatom *Chaetoceros calcitrans* under high nutrient concentrations. J Exp Mar Biol Ecol 446:67-75.

68. Agawin NSR, Duarte CM, Agustí S (2000) Nutrient and temperature control of the contribution of picoplankton to phytoplankton biomass and production. Limnol Oceanogr 45:591–600. doi: 10.4319/lo.2000.45.3.0591

69. Töpper B, Thingstad TF, Sandaa RA (2013) Effects of differences in organic supply on bacterial diversity subject to viral lysis. FEMS Microbiol Ecol 83(1):202-213. doi: 10.1111/j.1574-6941.2012.01463.x.

70. Sundareshwar P V, Morris JT, Koepfler EK, Fornwalt B (2003) Phosphorus limitation of coastal ecosystem processes. Science 299:563–565. doi: 10.1126/science.1079100.

71. Guerzoni S, Chester R, Dulac F, Herut B, Loye-Pilot M-D, Measures C, Migon C, Molinaroli E, Moulin C, Rossini P, Saydam C, Soudine A, Ziveri P (1999). The role of atmospheric deposition in the biogeochemistry of the Mediterranean Sea. Prog Oceanogr 44:147-190.71.

72. Carlsson P, Granéli E, Granéli W, Gonzalez Rodriguez E, Fernandes de Carvallo W, Brutemark A, Lindehoff E (2012). Bacterial and phytoplankton nutrient limitation in tropical marine waters, and a coastal lake in Brazil. J Exp Mar Biol Ecol 418-419:37-45. doi: 10.1016/j.jembe.2012.03.012.

73. Duarte CM, Agustí S, Gasol JM, Vaqué D, Vazquez-Dominguez E (2000) Effect of nutrient supply on the biomass structure of planktonic communities: an experimental test on a Mediterranean coastal community. Mar Ecol Prog Ser 206:87-95. doi: 10.3354/meps206087.

74. Lekunberri I, Lefort T, Romero E, Vázquez-Domínguez E, Romera-Castillo C, Marrasé C, Peters F, Weinbauer M, Gasol JM (2010) Effects of a dust deposition event on coastal marine

764 microbial abundance and activity, bacterial community structure and ecosystem function. J
765 Plankton Res 32(4):381-396.

766 75. Pulido-Villena E, Baudoux A-C, Obernosterer I, Landa M, Caparros J, Catala P, Georges C,
767 Harmand J, Guieu C (2014). Microbial food web dynamics in response to a Saharan dust event:
768 results from a mesocosm study in the oligotrophic Mediterranean Sea. Biogeosciences
769 11:5607-5619.

770

Figure & Table Captions

Fig. 1. Temporal changes in concentrations of NH_4 (a) and PO_4 (b), turnover time of PO_4 (PO_4 Tt: c), prokaryotic heterotrophic activity based on thymidine incorporation (d), prokaryotic heterotrophic activity based on leucine incorporation on Day 4 only (e) and total primary production (PP_t: f). Data are Mean ± SD of three replicates. K refers to the control incubations, N+ to NH_4 addition, P+ to PO_4 addition and NP+ to simultaneous NH_4 and PO_4 addition.

Fig. 2. Relationship between leucine and thymidine incorporation rates (in logarithmic scale) in the different treatments on the last day of the experiment. Data are Mean ± SD of three replicates. K refers to the control incubations, N+ to NH_4 addition, P+ to PO_4 addition and NP+ to simultaneous NH_4 and PO_4 addition. Also line 1/1.

Fig. 3. Responses of 0.2-2.0 (white), 2.0-5.0 (grey) and > 5.0 μm (black) size fractions of primary production in the different treatments on Day 0 (a) and Day 4 (b). Data are Mean ± SD of three replicates. K refers to the control incubations, N+ to NH_4 addition, P+ to PO_4 addition and NP+ to simultaneous NH_4 and PO_4 addition.

Fig. 4. Temporal changes in abundances of *Synechococcus* (a), *Prochlorococcus* (b), autotrophic pico eukaryotes (c), heterotrophic prokaryotes (HProk: d), viruses (VLP: e)**,** diatoms (f), dinoflagellates (g) and coccolithophores (h). Data are Mean ± SD of three replicates. K refers to the control incubations, N+ to NH_4 addition, P+ to PO_4 addition and NP+ to simultaneous NH_4 and PO_4 addition.

Fig. 5. Sub-groups of heterotrophic prokaryotes (HProk, upper plots): characterized by high (white) and low DNA content (grey) and sub-groups of viruses (VLP, lower plots): characterized by high (white), medium (dark grey) and low (light grey) DNA content, on Days 0 and 4, according to SYBR Green I fluorescence, in the different treatments. Data are Mean ± SD of three replicates. K refers to the control incubations, N+ to NH_4 addition, P+ to PO_4 addition and NP+ to simultaneous NH_4 and PO_4 addition. $HProk_{high}$ and $HProk_{low}$ refer to high- and low-DNA content Hprok, respectively. VLP_{high}, VLP_{medium} and VLP_{low} refer to high-, medium- and low-DNA content VLP, respectively.

Fig. 6. Cluster analysis of the DGGE gel bands of the prokaryotic community. C1t0 and C2t0 refer to the seawater used for filling the microcosms on Day 0, and K1-3 refer to the control incubations, N1-3+ to NH_4 addition, P1-3+ to PO_4 addition and NP1-3+ to simultaneous NH_4 and PO_4 addition on Day 4.

Fig. 7. DGGE profiles of prokaryotic 16S rRNA gene fragments for Day 0 K1 (K1') and K2 (K2') microcosms, as well as Day 4 K, N+, P+ and NP+ microcosms. K refers to the control incubations, N+ to NH_4 addition, P+ to PO_4 addition and NP+ to simultaneous NH_4 and PO_4 addition.

Table 1. Range, average values and abbreviations of all measured parameters in the seawater mass that was used for filling the microcosms on Day 0.

812 **Figure 1**

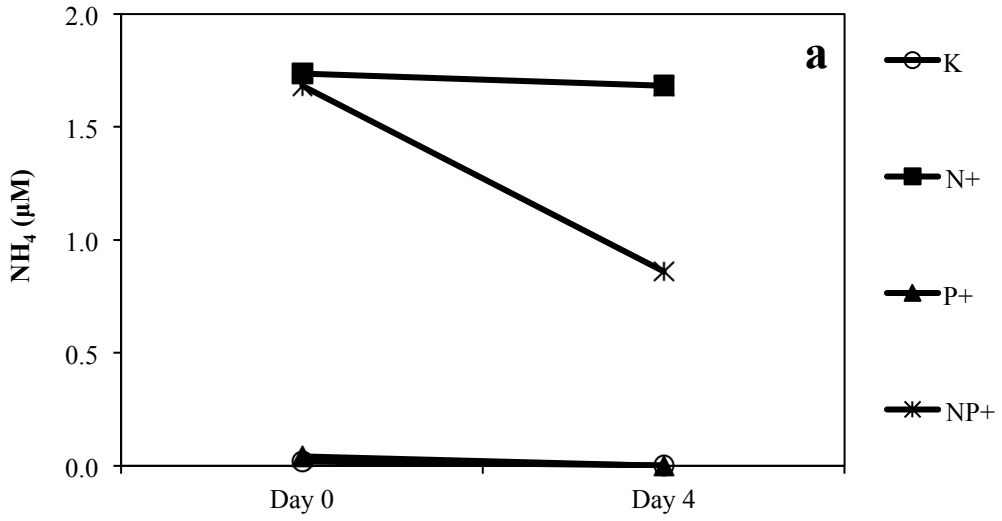

813

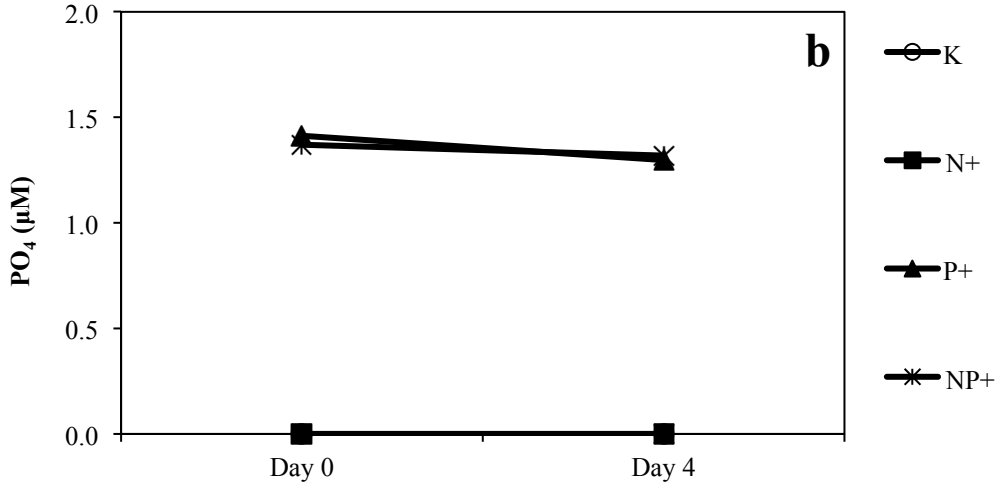

814

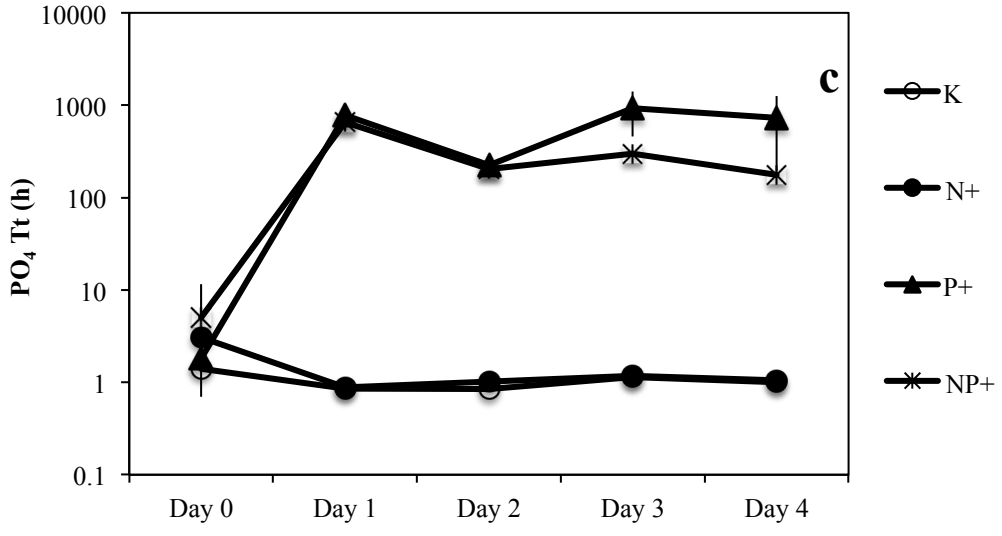

815

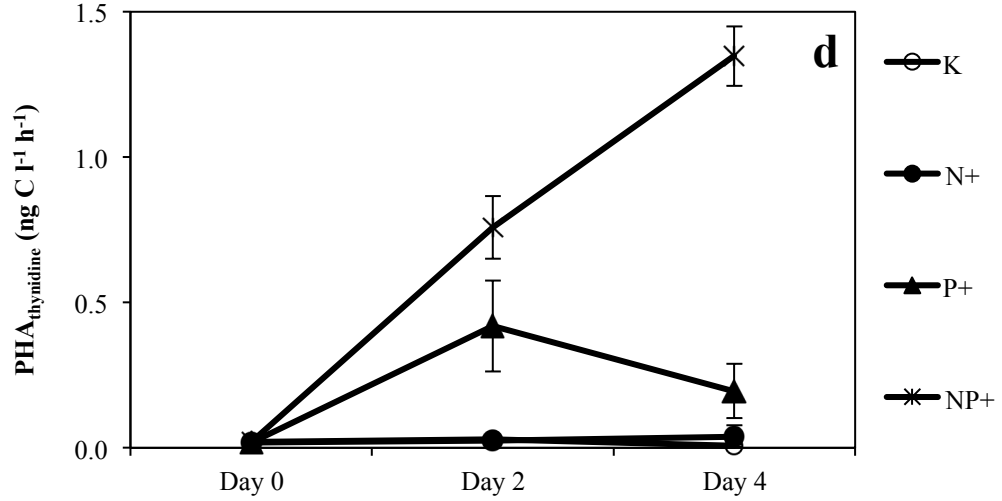

816

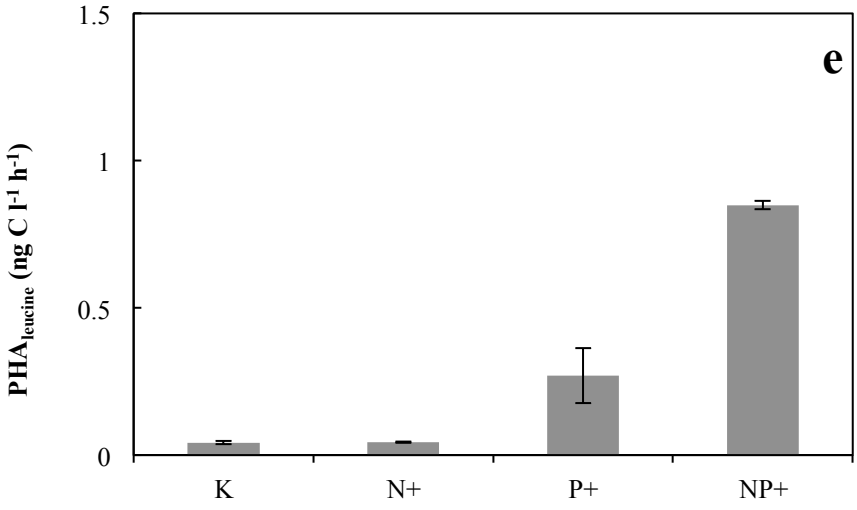

817

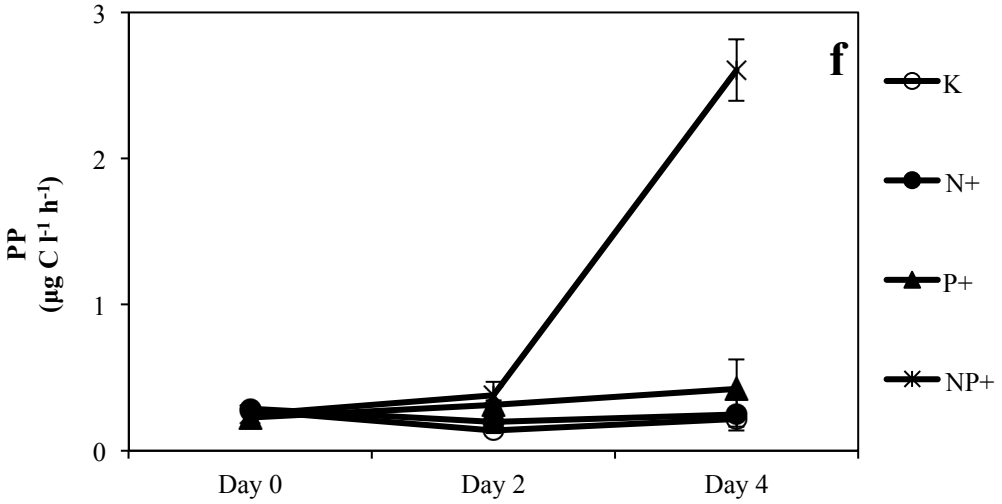

818

819

820 **Figure 2**

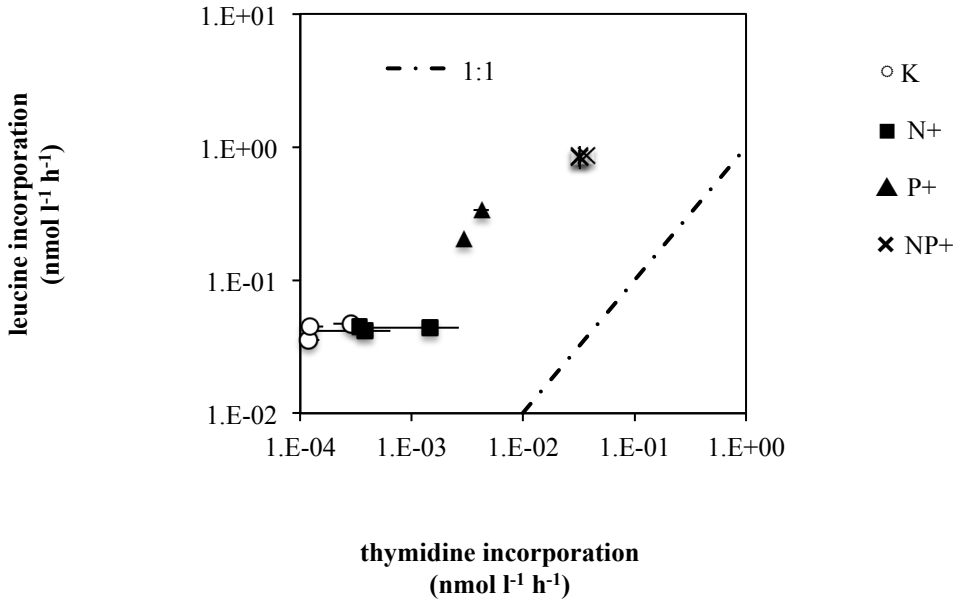

821

822 **Figure 3**

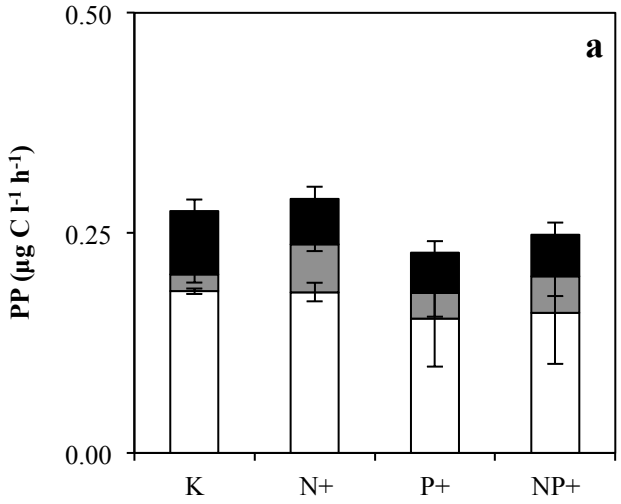

823

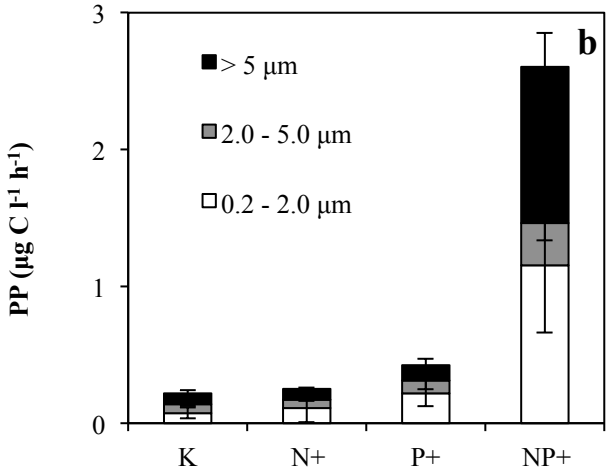

824

825 **Figure 4**

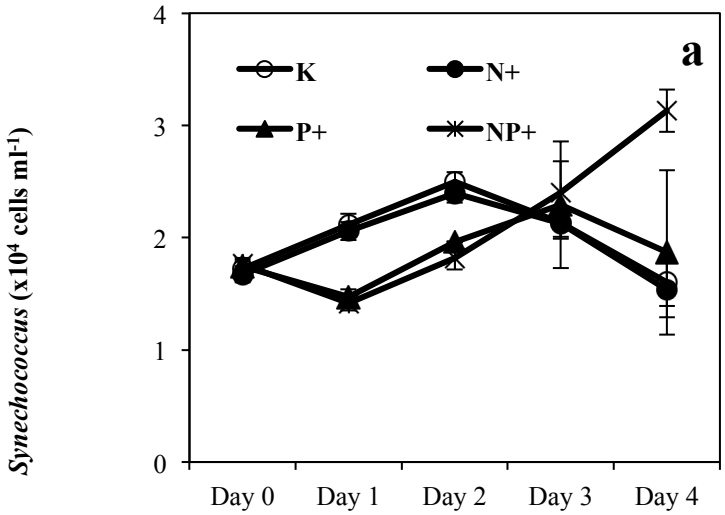

826

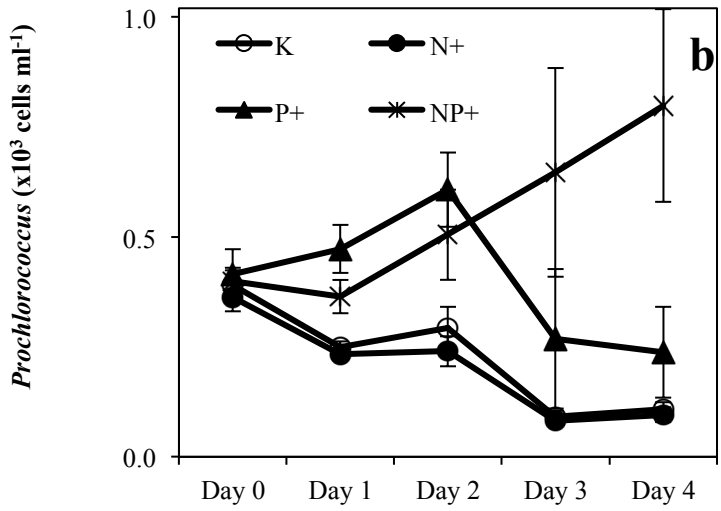

827

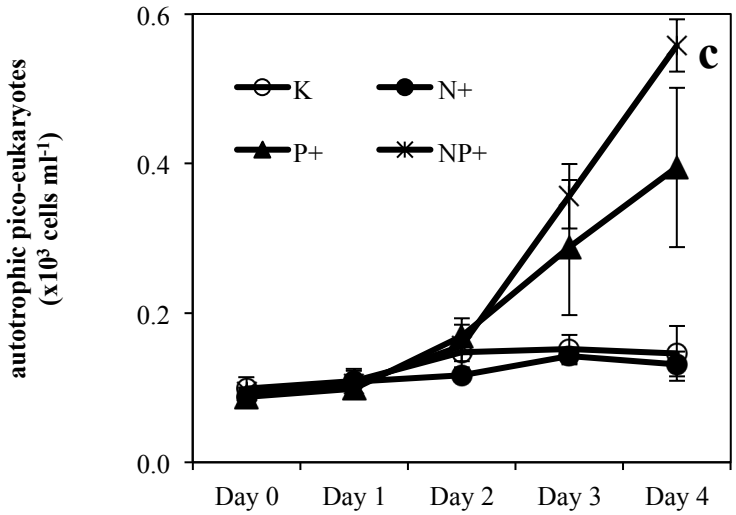

828

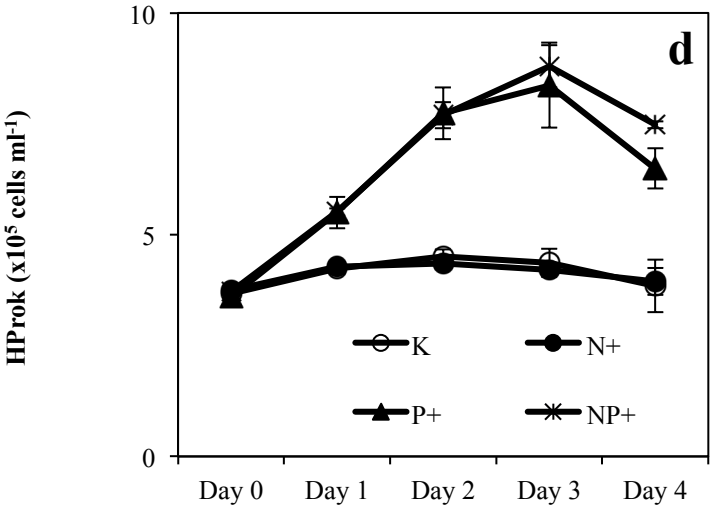
d
HProk (x10^5 cells ml^-1)
10
5
0
K
N+
P+
NP+
Day 0
Day 1
Day 2
Day 3
Day 4

829

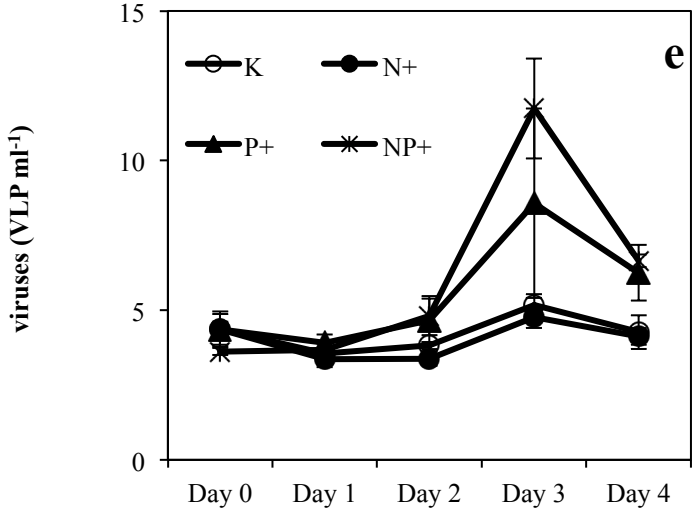
e
viruses (VLP ml^-1)
15
10
5
0
K
N+
P+
NP+
Day 0
Day 1
Day 2
Day 3
Day 4

830

831

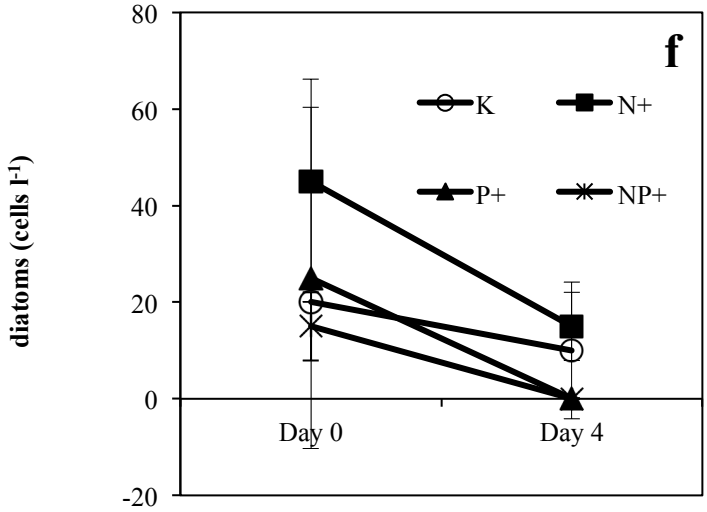
f
K
N+
P+
NP+
diatoms (cells l-1)
80
60
40
20
0
-20
Day 0
Day 4

832

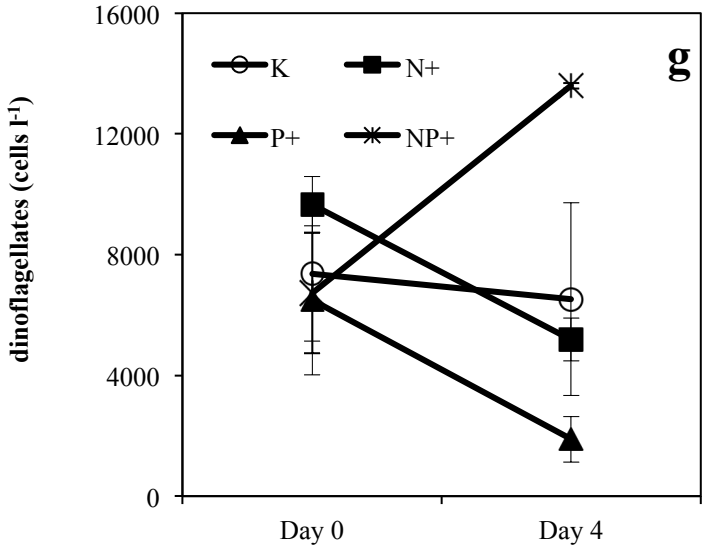
g
K
N+
P+
NP+
dinoflagellates (cells l-1)
16000
12000
8000
4000
0
Day 0
Day 4

833

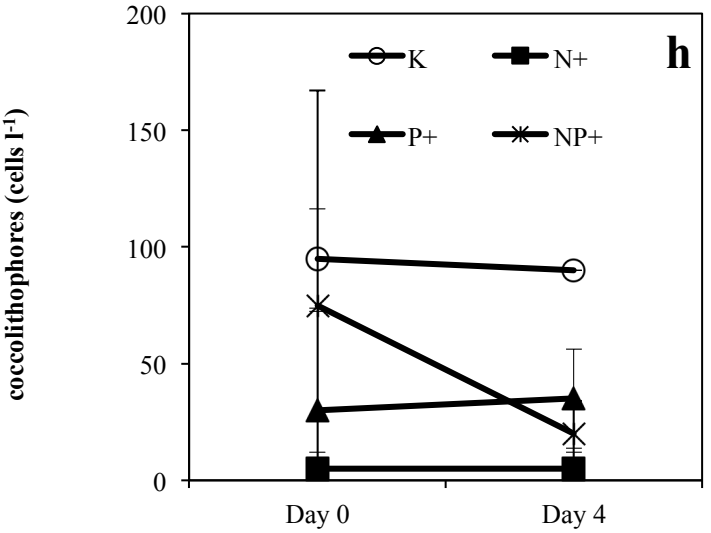
h
K
N+
P+
NP+
coccolithophores (cells l-1)
200
150
100
50
0
Day 0
Day 4

834

Figure 5

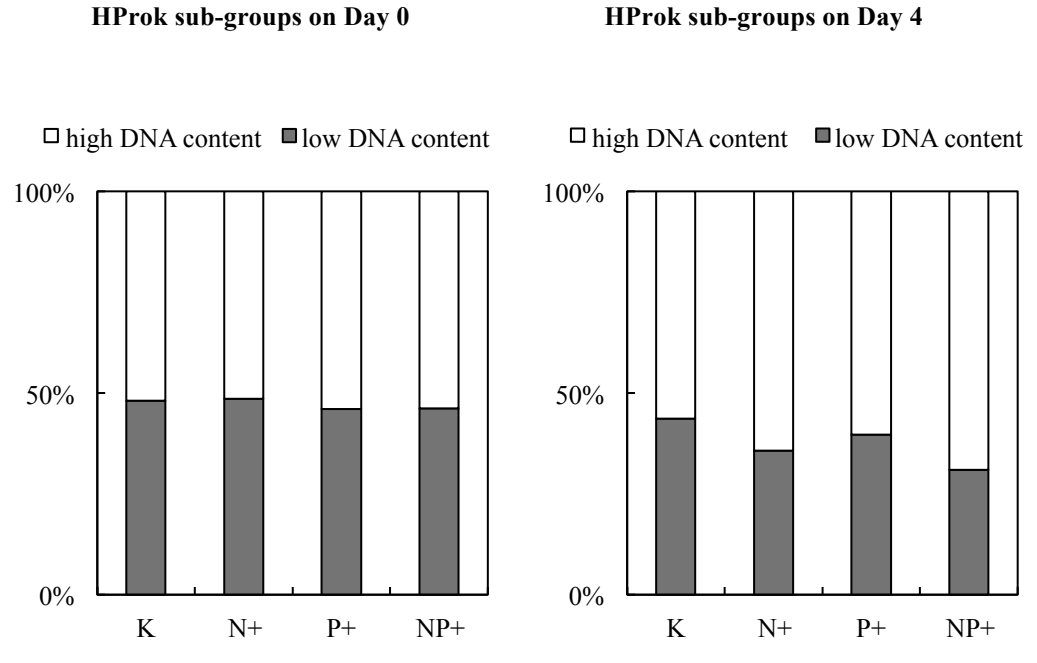
HProk sub-groups on Day 0
HProk sub-groups on Day 4
high DNA content
low DNA content
100%
50%
0%
K
N+
P+
NP+

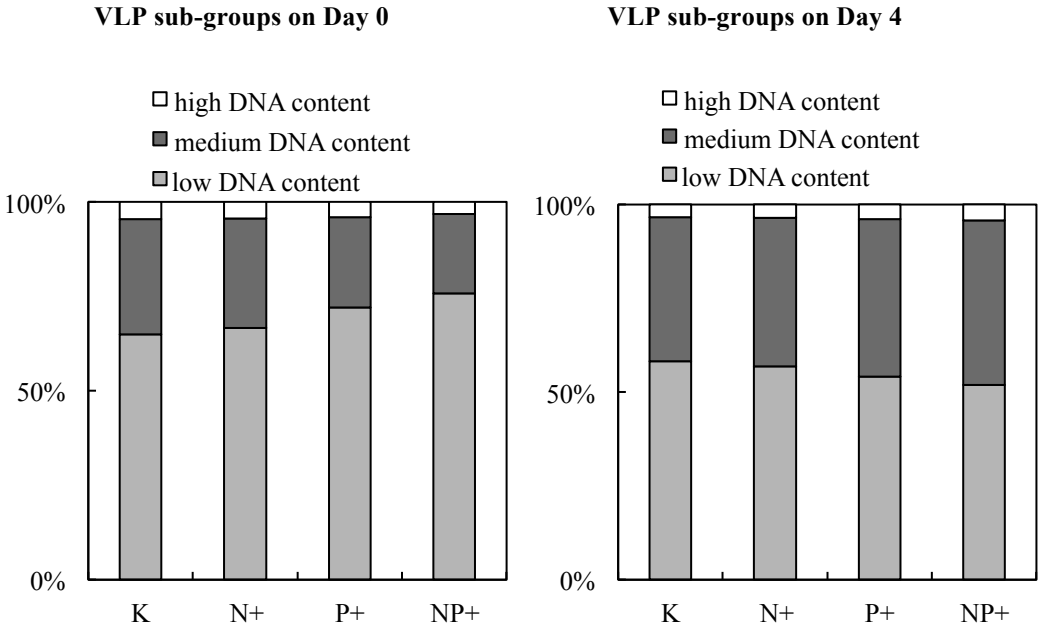
VLP sub-groups on Day 0
VLP sub-groups on Day 4
high DNA content
medium DNA content
low DNA content
100%
50%
0%
K
N+
P+
NP+

840 **Figure 6**

841

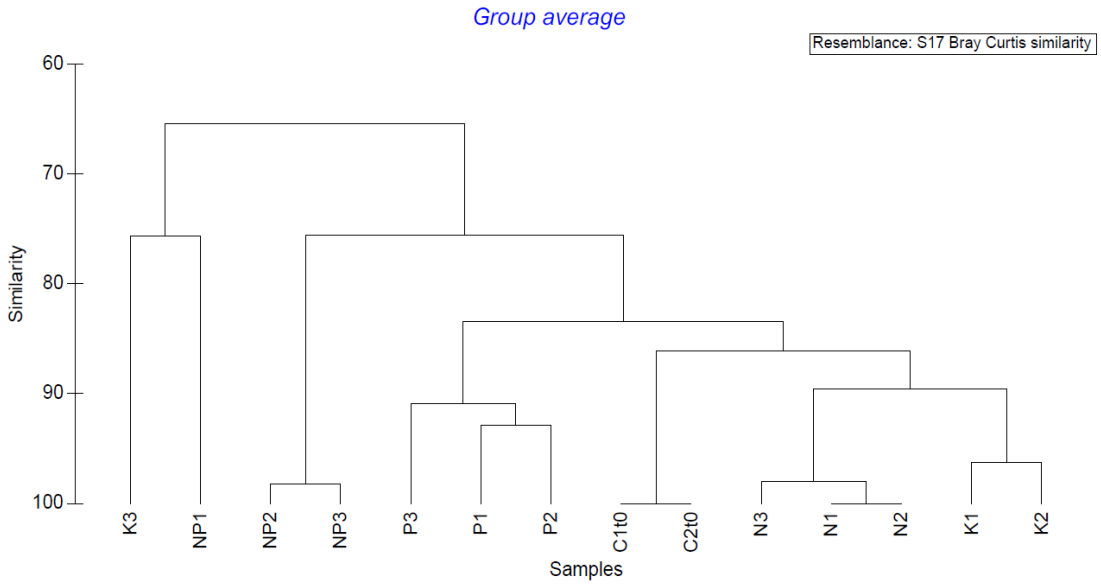

842

843

844 **Figure 7**

845 **K1 K2 K3 N1 N2 N3 P1 P2 P3 NP1 NP2 NP3 K1' K2'**

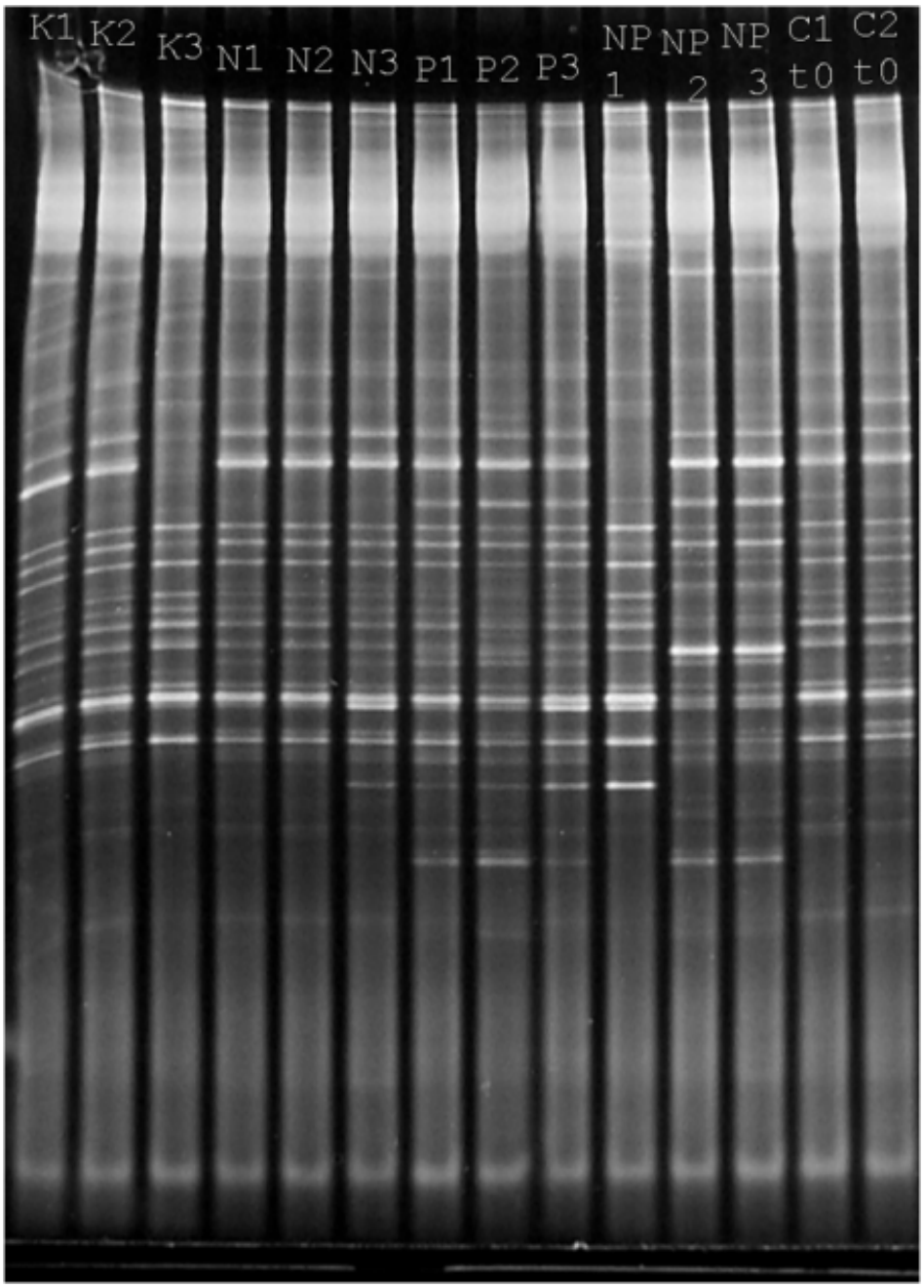

846

847